

Microwave Interactions of Laser Diodes and Modulators

Muhammed Al-Mumayiz

University College London and Agilent Technologies

Abstract: A review of various models for the laser diode, electroabsorption modulator (EAM), and the microwave interactions between them, is presented. A model of an integrated version of a laser and modulator, the electroabsorption modulated distributed feedback laser (EAM-DFB) will also be shown. Exploring the various ways in which the devices electrically interact with each other facilitates a clearer view of how these components function.

1 Introduction

High-speed lasers and modulators play an integral part in today's fibre-optic communication applications. The rapid increase in Internet traffic has forced these optical components to be able to handle greater bit rates.

A laser can be directly modulated by turning on and off its input drive current, but the laser will display transient oscillation at a frequency equal to its relaxation oscillation (resonant) frequency. As bit rates increase, the obvious problem would be that the oscillation might not have settled before the next bit comes along. Chirp is another problem arising in directly modulated lasers. As the input drive current of a laser changes, so does the carrier density, hence refractive index, and therefore wavelength. The laser wavelength moves in opposite directions respectively as the pulse rises and falls. The higher the bit rate, the more the chirp begins to manifest itself as an effective widening of the laser wavelength linewidth. This is quantified by the linewidth enhancement factor, which is desired to be as small as possible. Due to chromatic dispersion (different wavelengths travel at different velocities) in optical fibres, pulse spreading is most likely to occur in the case of a wider laser linewidth, thereby limiting the transmission distance.

It is possible to keep the laser in continuous wave (CW) operation, and modulate it externally. This would eliminate the aforementioned problem of transient oscillation, and hopefully reduce the chirp, providing the modulator suffers from less chirp than the laser. An electroabsorption modulator (EAM) is a viable option as an external modulator. Some of its advantages compared to other alternatives are: low cost, low drive voltages, small size, and the ability to be monolithically integrated with distributed feedback (DFB) or distributed Bragg reflector (DBR) lasers [1]. An EAM is based on a very similar structure to a laser, with the active layer and current-blocking regions present. The difference is that it is operated in reverse bias. As the input stream of data bits alters the modulator reverse bias, the absorption coefficient of the modulator changes. For instance, the modulator can be transparent to the light emitted from the laser for a zero bit, and opaque for a one bit (i.e. a certain amount of absorption is taking place).

It is important for models of lasers and modulators take into account the optical characteristics relating to the semiconductor physics of the device. It is however, very important to deduce the electrical model of the device, in order to understand more comprehensively its behaviour under various conditions. Generating an electrical model of a laser or modulator, followed by fitting to measured data and validation of the model, allows chip parasitics to be extracted. If the device is subsequently integrated into a package, and further measurements are taken, package parasitics can be determined. It is also very critical to observe and evaluate the parasitic interactions between the laser and modulator, particularly in a monolithic EAM-DFB. Without proper isolation between them, undesirable induced effects can occur. This paper reviews some of the modelling work done in this field, and introduces planned modelling work at Agilent.

2 Laser Modelling

Even though many laser models have been produced over the years, a complete model can be broken down into hierarchical levels, as shown in Figure 1.

The integrated equivalent circuit model [2] represents the laser in three levels. The intrinsic laser model (level 1) can be used to model the optical characteristics. This can be integrated with the parasitic model (level 2), thereby allowing extrinsic laser characteristics to be modelled. Finally, a

complete laser transmitter circuit model can be achieved by taking external circuits into account. This hierarchical approach can be conveniently accommodated into CAD packages such as Agilent EESoft ADS.

The intrinsic laser is represented with the laser rate equations, the core of the laser model. These two differential equations illustrate a coupling between the electron and photon populations within the active layer. Under large signal conditions, nonlinear effects, such as optical output power saturating with increasing input drive current and temperature, begin to take hold. Using nonlinear modelling simulators such as SPICE allows these effects to be represented, albeit with some difficulty.

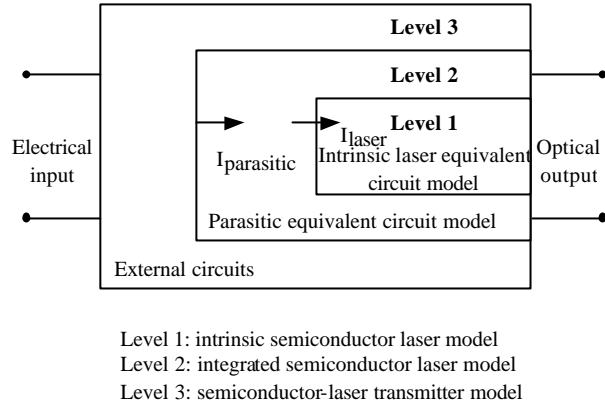


Figure 1: Hierarchical representation of laser equivalent circuit [2]

Investigations have tried to pinpoint the origins of parasitic roll-off in a laser frequency response [3], which is characterised by an RC network. It is obviously desirable to find out the source of the effective resistance and capacitance in order to devise ways to reduce them, thereby increasing the bandwidth. Even though some of these parasitic high frequency current paths have complicated origins, a simplistic approach can be used to model the chip and package parasitics (Figure 2). The chip parasitics consist of the bondpad capacitance, and the stray capacitance and resistance originating from the p and n blocking regions encapsulating the active layer. These can be schematically represented by C_s , the effective shunt parasitic capacitance (usually dominated by the largest parallel capacitance), and R_s , the effective resistance in series with the intrinsic laser. I_L represents the current leakage around the active layer. The package parasitics tend to comprise the bond-wire inductance and the small capacitance between the package input terminals. L_p and R_p can represent the bondwire inductance and resistance respectively, while C_p is the input terminal capacitance. I_s represents the current driving the laser, and R_{in} is the resistance of the laser driver, be it a signal generator (lower R_{in}) or transistor (higher R_{in}) for instance. I_A is the current injected into the laser active layer.

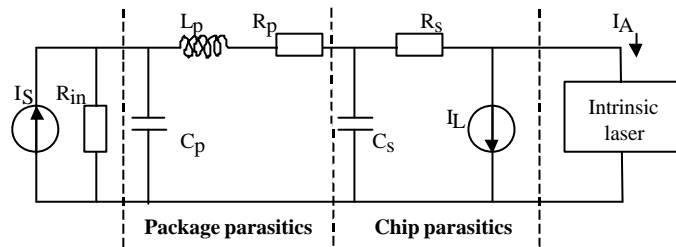


Figure 2: Circuit model showing package and chip parasitics [3]

More recent lasers have reduced parasitic capacitance by isolating the bondpad from the active stripe using trenches. Recently at Agilent, a SPICE-based diode model enabled the parasitic capacitance of the blocking junctions to be dependent on different drive levels [4]. As in previous work, bondpads may be modelled using simple capacitors. Accurate modelling in a large signal regime has been demonstrated using p-n junction diodes to realistically simulate current leakage around the active region. This is where the significance of drive-dependent capacitance in the diode model is used to best effect.

3 Modulator Modelling

One of the earlier EAM models [5] realises a simple RF equivalent circuit model by extracting circuit parameters from measured S_{11} values, and includes the effect of optical power to the E/O response and also device impedance. The EAM photocurrent is represented by a current path rather than a current source. This current path impedance is represented by a resistance $R_o = \frac{dV_j}{dI_o}$ (Figure 3), where I_o is the

EAM DC photocurrent and V_j the junction DC voltage. C_j represents the junction capacitance, R_s is the device series resistance. The EAM E/O frequency response is determined from the ratio of C_j AC voltage to modulator input AC voltage. The strength of this model depends on the small number of parameters needed (three) that can accurately model the EAM. Although all these parameters can be found via microwave S_{11} measurements, conventional low frequency methods can also be used to individually calculate or measure them. C_j can be found with CV measurements or using parallel-plate capacitor measurements. R_s can be found by measuring the slope of the forward I-V curve at large current, or by estimating the electrode ohmic contact resistance together with the semiconductor layers' bulk resistance. An approximation of R_o can be obtained from the slope of the reverse I-V curve with the EAM subject to an optical input. R_o is proportional to the optical power prior to the onset of DC saturation. Analysing the EA characteristics enables the theoretical relationship between EAM photocurrent and reverse bias voltage to be established, and allows R_o to be determined as well.

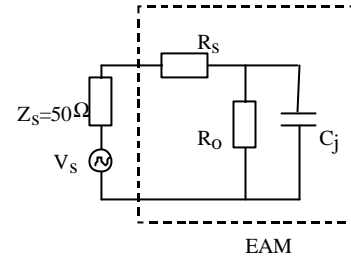


Figure 3: RF equivalent circuit model for lumped element EAM [5]

Investigations have been made into a large-signal dynamic model of an integrated EAM-DFB using the time-dependent transfer matrix method (TMM) [6]. Conventional TMM can only estimate the static characteristics of optical semiconductors, whereas the time-dependent version can estimate the dynamic characteristics. The laser and EAM chirp can be calculated separately in addition to the grating phase at the end of the laser section, the length of the waveguide region, and electrical coupling. Figure 4(a) portrays the EAM-DFB structure, while Figure 4(b) illustrates wave propagation in EAM-DFB lasers.

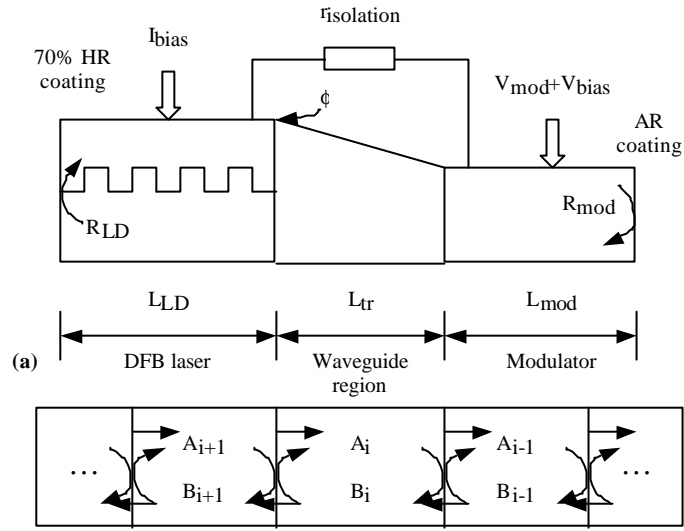


Figure 4: (a) Cross-sectional schematic of EAM-DFB; (b) schematic illustrating wave propagation on time-dependent TMM-based large signal dynamic EAM-DFB laser model [6]

It is possible for time-dependent TMM to not only involve forward travelling waves, but also backward reflected waves. This includes the ability to consider spatial hole burning since the overall structure is split into smaller sections. It is very important to calculate the correct spacing of each section, though, because inaccuracies can result.

4 Microwave Interactions

In integrated EAM-DFB devices, it is critical to evaluate the interactions between the devices. Electrical isolation between the laser and EAM is very important, since if the isolation resistance is small, and as the modulator bias voltage increases, several detrimental effects can occur [7]. There is a considerable decrease of injection current to the laser, an increase of threshold current, a decrease of laser output, a change of laser wavelength, and a leakage current to the laser section, leading to a reduction of effective applied voltage to the modulator waveguide. Other problems can occur at RF modulation frequencies. The spectrum measured at the modulator facet displayed asymmetric sidebands to the carrier frequency. This asymmetry depends on the modulation frequency and laser diode injection current. However, symmetric sidebands appeared in the spectrum measured at the laser facet. This implies a small direct modulation occurring in the DFB laser. This is most likely to be caused by an induced RF signal from the modulator via the bonding wires and by the modulated reflected light from the modulator facet. This unwanted additional modulation of the laser was largest

at a frequency coinciding with the laser relaxation oscillation frequency. Suzuki et al. [7] showed that these adverse effects could be eliminated by placing a bypass capacitor in parallel with the laser and by depositing an AR coating (SiN) onto the modulator facet. The static wavelength shift resulting from modulator bias change remained as a problem, and it was proposed that this could be rectified by more deeply investigating the optical coupling between laser and EAM, in addition to DFB design parameters such as coupling coefficient (κL). Removing the aforementioned discrepancies resulted in an improved frequency response of the integrated device. Even the linewidth enhancement factor was reduced due to elimination of the additional unwanted laser diode modulation.

Subsequent research has investigated how modulator current leakage can influence laser wavelength [8]. Firstly, it can cause dynamic (or transient) chirp in the laser, since a change in modulator bias voltage will lead to a small fraction of current being shunted through the laser. Secondly, adiabatic (low frequency) chirp can be induced into the laser, because the laser wavelength shift can also be caused by a change in laser DC drive current. It is possible to determine a minimum value for the laser-to-modulator isolation resistance for each kind of chirp, and select the higher of the two resistance values.

5 Conclusion and Future Work

A brief exploration into various laser and modulator models has been provided. The microwave interactions between the devices have been assessed. It will be hoped that a model for EAMs can be further investigated, possibly supplemented by an examination into new technologies such as travelling-wave electroabsorption modulators (TWEAM). These devices can achieve higher bit rates, and a greater bandwidth-length product than the lumped equivalent [9]. This is due to a mitigation of an RC-limited bandwidth. Currently though, they still display high electrical and optical loss. It will also be quite useful to investigate new driver circuit technologies and assess all the interactions between driver, laser, and modulator.

Acknowledgements

The author would like to thank all the supervisors involved for help and encouragement. He would also like to thank the advice offered by employees at Agilent Technologies Ipswich Components Operation, particularly Dr. Mark Holm, whose guidance has proven very valuable in understanding many advanced concepts, and for allowing the author to utilise information from an as-yet-unreleased paper [4]. The author is very grateful for the funding provided by EPSRC and Agilent Technologies under the Engineering Doctorate programme. Most importantly, the author would like to thank his mother for always providing endless support and encouragement.

References

- [1] B.Mason, A. Ougazzaden, C.W. Lentz, K.G. Glogovsky, C.L. Reynolds, G.J. Przybylek, R.E. Leibenguth, T.L. Kercher, J.W. Boardman, M.T. Rader, J.M. Geary, F.S. Walters, L.J. Peticolas, J.M. Freund, S.N.G. Chu, A.Sirenko, R.J. Jurchenko, M.S. Hybertsen, L.J.P. Ketelsen, G. Raybon, "40-Gb/s tandem electroabsorption modulator," *IEEE Photonics Technology Letters*, vol. 14, no. 1, pp. 27-29, January 2002.
- [2] K.C. Sum, N.J. Gomes, "Microwave-optoelectronic modelling approaches for semiconductor lasers," *IEE Proceedings in Optoelectronics*, vol. 145, issue 3, pp. 141-146, June 1998.
- [3] R.S. Tucker, "High-speed modulation of semiconductor lasers," *IEEE Journal of Lightwave Technology*, vol. LT-3, no. 6, pp. 1180-1192, December 1985.
- [4] M.A. Holm, S. Aboulhoda, G.M. Berry, "Modeling the device parasitics of trench buried heterostructure laser diodes," submitted to *IEEE LEOS 2002*.
- [5] G.L. Li, P.K.L. Yu, W.S.C. Chang, K.K. Loi, C.K. Sun, S.A. Pappert, "Concise RF equivalent circuit model for electroabsorption modulators," *Electronics Letters*, vol. 36, no. 9, pp. 818-820, 27 April 2000.
- [6] Y.Kim, H.Lee, J. Lee, J. Han, T.W. Oh, J. Jeong, "Chirp characteristics of 10Gb/s electroabsorption modulator integrated DFB lasers," *IEEE Journal of Quantum Electronics*, vol. 36, no. 8, pp.900-908, August 2000.
- [7] M. Suzuki, H. Tanaka, S. Akiba, Y. Kushihiro, "Electrical and optical interactions between integrated InGaAsP/InP DFB lasers and electroabsorption modulators," *IEEE Journal of Lightwave Technology*, vol. 6, no. 6, June 1988.
- [8] R.A. Salvatore, R.T. Sahara, M.A. Bock, I. Libenzon, "Electroabsorption modulated laser for long transmission spans," *IEEE Journal of Quantum Electronics*, vol. 38, no. 5, May 2002.
- [9] S. Irmscher, R. Lewén, U. Eriksson, "InP-InGaAsP high-speed traveling-wave electroabsorption modulators with integrated termination resistors," *IEEE Photonics Technology Letters*, vol. 14, no. 7, July 2002.

The author is with University College London, Dept. of Electronic & Electrical Engineering, Torrington Place, London WC1E 7JE, and Agilent Technologies UK Ltd., White House Road, Ipswich, Suffolk IP1 5PB.